TABLE IV The resistivity ratio ρ_F/ρ_0 as evaluated from exact Equation 1. The values for $\mu \geqslant 20$ and $\alpha = 40$ are not reported because of inaccuracies in the numerical work (performed with a pocket calculator)

μ	$\alpha = 0.04$	$\alpha = 0.4$	$\alpha = 4$	$\alpha = 40$
0.8	1.40786	1.41217	1.46091	1.46907
1	1.33337	1.33661	1.37024	1.37522
2	1.17536	1.17655	1.18646	1.18710
4	1.09042	1.09080	1.09351	1.10472
10	1.03693	1.03700	1.03744	1.00074
20	1.01860	1.01862	1.01895	–
40	1.00932	1.00934	1.00800	–
100	1.00347	1.00374	1.01066	–

in terms of complicated models evoking either the anisotropy of the energy surface [10] or two overlapping energy bands of spherical symmetry [11, 12].

Similar behaviour can be predicted when the grain-boundaries act as efficient scatterers, since the Fuchs–Sondheimer (F–S) conduction model can then be replaced by an effective F–S model [13–15] which leads to the same form of equations, as previously shown [14, 15]. However detailed calculations are difficult and are not so easy to interpret as those in the F–S model; this point will be discussed in a future communication.

It can then be theoretically predicted that any experimental observation of the magnetoresistance effect in relatively thick films cannot be attributed to the usual size effect induced by geometrical limitation in the mean free path, but could be due to properties of energy surface [10] or energy bands [12] or to impurities [16].

References

1. C. R. TELLIER, M. RABEL and A. J. TOSSER, *J. Phys. F: Met. Phys.* 8 (1978) 2357.
2. A. A. COTTEY, *J. Phys. F: Met. Phys.* **2** (1972) 625.
3. A. A. COTTEY, *Thin Solid Films* **1** (1967/68) 297.
4. E. H. SONDHEIMER, *Phys. Rev.* **80** (1950) 401.
5. G. C. JAIN and B. S. VERMA, *Thin Solid Films* **15** (1973) 15.
6. C. R. TELLIER and A. J. TOSSER, *Rev. Phys. Appl.* **13** (1978) 441.
7. K. L. CHOPRA, "Thin Film Phenomena" (McGraw-Hill, New York, 1969).
8. K. FORSVOLL and I. HOLWECH, *Phil. Mag.* 9 (1964) 435.
9. *Idem, ibid.* 9 (1964) 921.
10. J. M. ZIMAN, "Electrons and Phonons" (Oxford University Press, London, 1963) Ch. XII.
11. E. H. SONDHEIMER and A. H. WILSON, *Proc. Roy. Soc. A* **190** (1947) 435.
12. *Idem, ibid.* **193** (1948) 484.
13. T. J. COUTTS, *Thin Solid Films* 7 (1971) 77.
14. C. R. TELLIER, C. BOUTRIT and A. J. TOSSER, *ibid.* 44 (1977) 201.
15. C. R. TELLIER, *ibid.* **51** (1978) 311.
16. C. M. HURD, "The Hall effect in Metals and Alloys" (Plenum Press, London, 1972).

Received 15 July
and accepted 1 August 1980

C. R. TELLIER*
A. J. TOSSER
C. R. PICHARD
Laboratoire d'Electronique,
Universite de Nancy 1,
CO 140-54037 Nancy, France

*Present address: Laboratoire de Chronométrie et Piézoelectroicité, ENSMM, Route de Gray, 25030 Besançon Cedex, France.

Some comments on ceramic solid-state reaction kinetics using results obtained on the ZnO–Al_2O_3 system

Ceramic solid-state reactions are usually carried out by intimately mixing fine powders and then firing them at high temperatures. When the reactions proceed isothermally it has been found [1, 2] that a number of diffusional models, namely those of Jander, Dünwald–Wagner, Valensi, Carter, Zhuravlev–Lesokhin–Tempel'man, Ginstling–Brounshtein and Kröger–Ziegler, hold for many ceramic solid-state reactions. Although these models show differences they all assume particles of uniform radius surrounded by a second reactant and an interface layer of uniform thickness growing with time. The ZnO–Al_2O_3 system has appeared to be an interesting system for checking the validity of these models. Indeed, ZnO and Al_2O_3 combine to form a unique stable compound $ZnAl_2O_4$ of normal spinel structure at moderately high temperatures (600 to 1400° C) and it has been demonstrated that the overall reaction process can be seen as a one-way transfer of zinc

 © *1981 Chapman and Hall Ltd.*

TABLE I Raw materials used for preparing the $ZnO-Al_2O_3$ mixtures

Material	Grade	Grain size distribution	Specific area* ($m^2 g^{-1}$)
ZnO†	UCB	Used as-received	4.2
Al_2O_3 (I)‡	Tabular Alcoa T.60	Prepared by water sieving between 74 and 37 μm of an as-received < 48 mesh	0.15
Al_2O_3 (II)‡	Tabular Alcoa T.60	Used as-received < 325 mesh	0.83
Al_2O_3 (III)‡	Tabular Alcoa T.60	Prepared by BAHCO separation (< 5 μm) of an as-received < 48 mesh	0.89
Al_2O_3 (IV)†	Reactive Alcoa A15 SG	Used as-received	5.9

*The specific areas were measured using a dynamic BET method.
†More than 99.5 wt % purity.
‡More than 99 wt % purity, low iron content.

to the alumina grains with the reaction proceeding only on the alumina grains. $ZnO-Al_2O_3$ solid-state reaction results which are in agreement with the above models may be found in the literature [1, 2]. In previous work [3] it has been shown that during reaction between fine ZnO and Al_2O_3 of a similar grain size an expansion of the material occurs (inverse solid-state reaction sintering). Data on the kinetics of reaction expansion have been tentatively correlated and it appears that the chemical reaction generates an increase in the volume of the pores, due to geometrical effects. In order to establish the above mentioned quantitative correlation several hypotheses [3] were employed; one of them was that the zinc aluminate spinel forms as layers on the alumina grains at each point of contact (between alumina and zinc oxide grains) according to an angle of aperture of 2θ. The present work reports some results obtained by studying the reaction between different Al_2O_3 powders and ZnO. The interpretation of the results leads us to comment on solid-state reaction kinetics models.

The raw materials (listed in Table I) used were one part ZnO powder and four parts Al_2O_3 powder (one reactive and three tabular aluminas of the same grade).

The grain-size distributions were measured using a Micromeritics Sedigraph and results are presented at Fig. 1. Using these results and a spherical particle hypothesis the total number of particles in each powder, as well as the ratio of the number of particles of ZnO to Al_2O_3 ($N_{ZnO}/N_{Al_2O_3}$), has been calculated. These give $\simeq 5 \times 10^5$ for alumina (I); $\simeq 300$ for alumina (II); $\simeq 3$ for alumina (III); and $\simeq 0.4$ for alumina (IV). Exper-

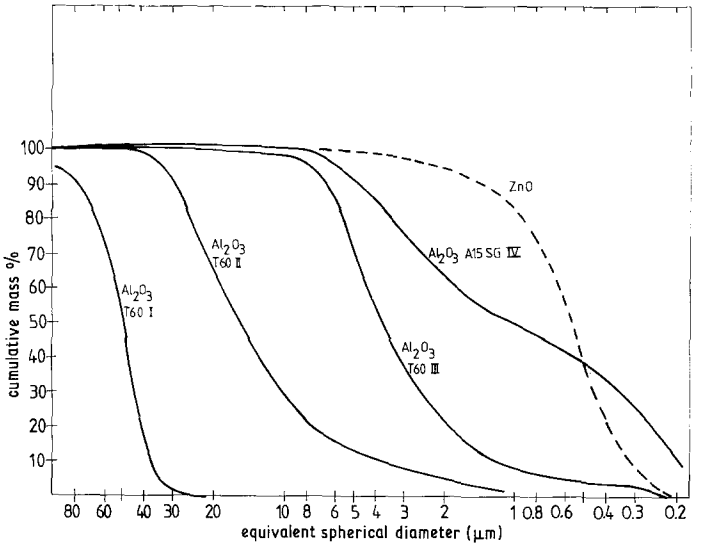

Figure 1 Grain-size distributions of ZnO and Al_2O_3 powders.

TABLE II Firing temperatures of $ZnO-Al_2O_3$ mixtures

$ZnO-Al_2O_3$ mixtures	Firing temperature (° C)						
	900	950	1000	1100	1200	1300	1400
Al_2O_3 (I)	–	–	X	X	X	–	–
Al_2O_3 (II)	–	–	X	–	X	–	–
Al_2O_3 (III)	–	–	X	–	X	–	–
Al_2O_3 (IV)	X	X	X		X	X	X

imental details (mixing, shaping, drying, firing, determination of $ZnAl_2O_4$ content, porosity measurements) are similar to those previously described [3]. The firing temperatures for $ZnO-Al_2O_3$ mixtures are listed in Table II.

It should be noted that all samples prepared from the various $ZnO-Al_2O_3$ mixtures expand during reaction. Results on the expansion phenomena are not considered here.

Figs 2, 3 and 4 illustrate the variation of the molar fraction (α) of the spinel phase formed with time; α being defined as $\alpha = n_s/(n_A + n_Z + n_S)$ where n_A, n_Z and n_S are the number of moles of Al_2O_3, ZnO and $ZnAl_2O_4$, respectively. The kinetic results obtained with the $ZnO-Al_2O_3$ (IV) mixtures are presented in Fig. 2. Examination of the graphs shows that the formation of the spinel phase is very rapid during the first hour of firing when α is equal to 49, 53, 70, 83, 91 and 93 mol% at 900, 950, 1000, 1200, 1300 and 1400° C, respectively. After the reaction rate decreases, the molar fraction seems to tend to a limit at each temperature. Such behaviour, in two marked stages, does not fit the classical diffusional models quoted in the introduction. It can best be understood by considering, as in a previous paper [3], that the reaction proceeds at each point of contact between grains according to a given angle (depending on the grain size radii) in which the spinel phase forms and grows.

Figs 3 and 4 make it possible to compare the reactional behaviour of the four aluminas at 1000 and 1200° C. It appears that the reaction rate is higher and the classical diffusional behaviour is less marked when the grain size is small and the temperature is high. Indeed reactive alumina (IV) and tabular alumina (III), which have grain size diameters and number of grains close to those of ZnO show, as already mentioned, a kinetic curve broken after 1 h of firing. In contrast, alumina (I), which can be considered as completely surrounded by ZnO grains (the number of Al_2O_3 grains being $\simeq 5 \times 10^5$ less than the number of ZnO grains) presents a much more conventional diffusional kinetic curve and the results satisfy the well known Valensi [4] equation at 1000 and 1100° C,

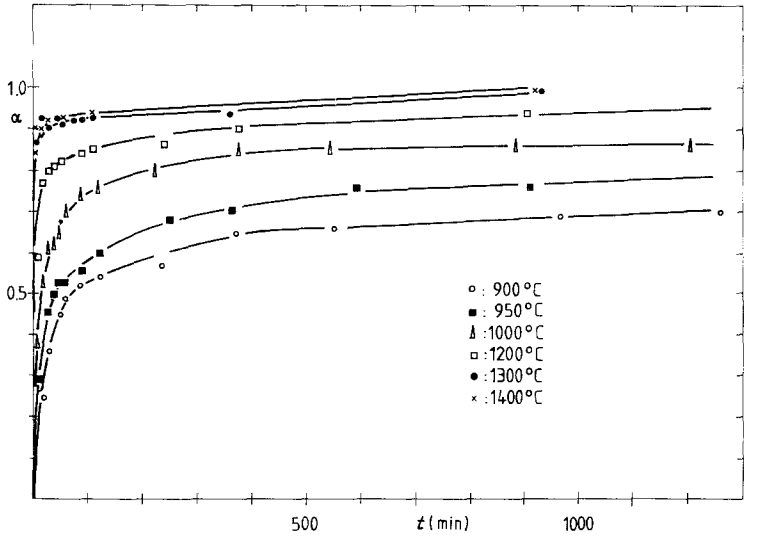

Figure 2 Evolution of the molar fraction of $ZnAl_2O_4$ against firing time for the $ZnO-Al_2O_3$ (IV) mixtures at different temperatures.

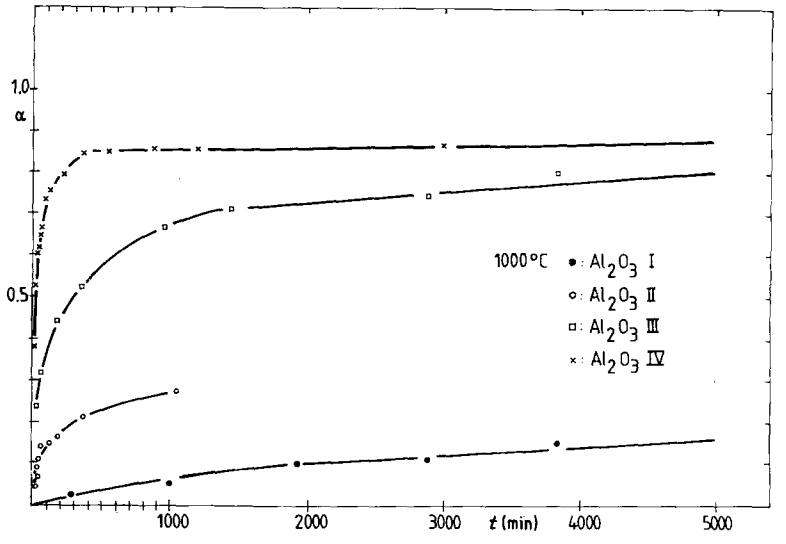

Figure 3 Evolution of the molar fraction of $ZnAl_2O_4$ against firing time for the four powder mixtures at 1000° C.

as shown in Figs 5 and 6. The activation energy (Arrhenius) calculated from the results has been found to equal 53 kcal mol^{-1} which is close to 57.5 kcal mol^{-1} quoted in the literature [2]. At 1200° C, the Valensi equation is no longer applicable. It should be remembered that at 1200° C the vapour pressure [5] of ZnO is high (10^{-1} torr at 1172° C, 1 torr at 1319° C) and it can be assumed that the reaction between ZnO and Al_2O_3 proceeds by the simultaneous action of solid-state and evaporation–condensation mechanisms. This leads to the following comments.

As noted in the introduction, conventional solid-state kinetic models assume particles of uniform radius surrounded by a second reactant. When the reaction proceeds only by solid-state diffusion this means that one particle of one kind must be completely surrounded by particles of the other kind. We attempt to illustrate this point by some geometrical considerations. Fig. 7 shows one spherical grain of kind (2) in contact with spherical grains of kind (1) of smaller diameter. The plane angle from which a smaller grain can be seen from the centre of the bigger grain is 2θ with

$$\theta = \arcsin \frac{d_1/d_2}{(1 + d_1/d_2)}, \qquad (1)$$

where d_1 and d_2 are the diameters of the respective grains. The solid angle ϕ of the cone of aperture

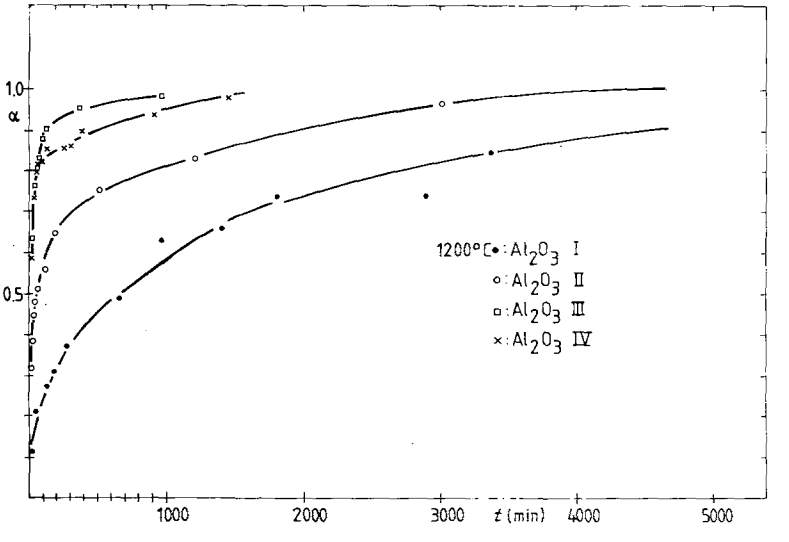

Figure 4 Evolution of the molar fraction of $ZnAl_2O_4$ against firing time for the four powder mixtures at 1200° C.

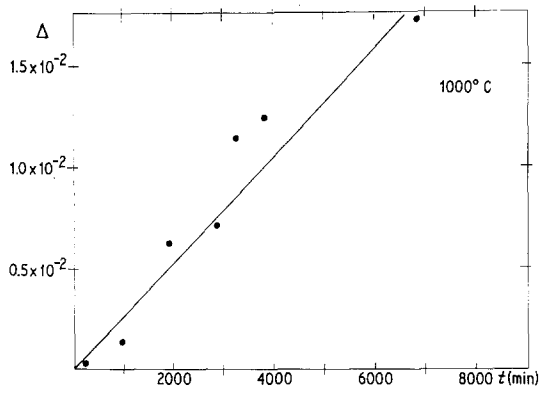

Figure 5 Illustration of the validity of the Valensi equation at 1000° C for $ZnO-Al_2O_3$ (I): Δ against firing time, with

$$\Delta = \frac{Z}{(Z-1)}\sqrt[3]{(1-x)^2} \frac{Z}{(Z-1)}\sqrt[3]{[1+(Z-1)x]^2} = Kt$$

where Z is the volume expansion, x is the advancement degree of the reaction ($x = 2\alpha/(1+\alpha)$) and K is the kinetic constant.

θ is equal to: $\phi = 2\pi(1-\cos\theta)$ steradians. By assuming that grains in a perfect mixture take up a random close packing of spheres geometry, the most probable co-ordination number $\bar{C}_c$ can be approximated [6] as

$$\bar{C}_c = 3 + 3.16\left(\frac{d_2}{d_1}\right)^2. \qquad (2)$$

So if a "coefficient of surrounding", S, is defined as the fraction of the solid angle occupied by the small grains on the bigger grain:

$$S = \frac{\bar{C}_c \cdot \phi}{4\P} \qquad (3)$$

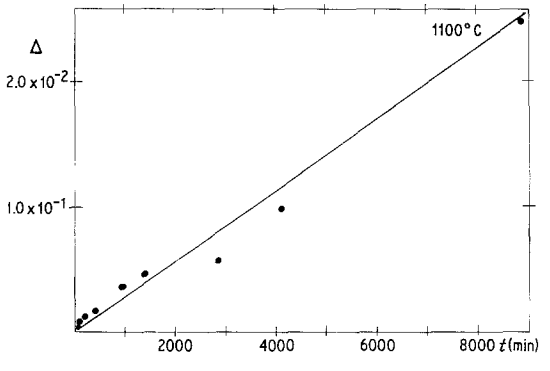

Figure 6 Illustration of the validity of the Valensi equation at 1100° C for $ZnO-Al_2O_3$ (I): Δ against firing time.

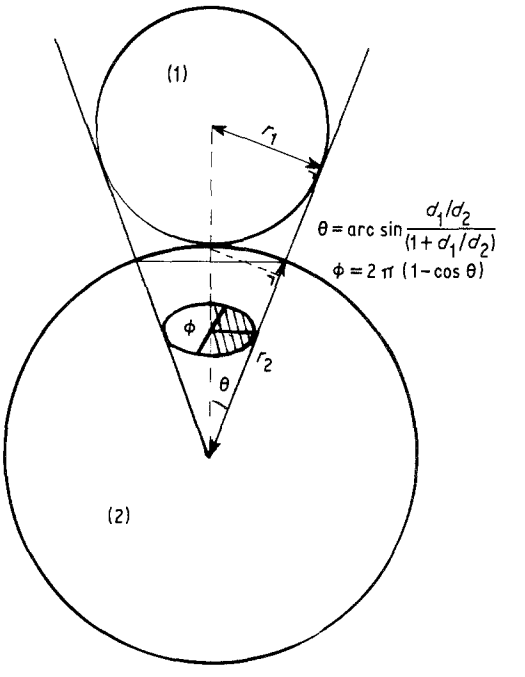

Figure 7 Geometrical characteristics of a bigger spherical grain (2) surrounded by smaller grains (1).

or

$$S(\%) = 50\left[3 + 3.16\left(\frac{d_2}{d_1}\right)^2\right] \times \left[1 - \cos \text{arc} \sin \frac{d_1/d_2}{(1+d_1/d_2)}\right].$$

$S(\%)$ has been plotted against d_1/d_2, as shown in Fig. 8. It should be pointed out that if $d_1 \ll d_2$, S tends to 79% which appears to be the maximum value of the "coefficient of surrounding". Examination of Fig. 8 shows that S stays very close to 79% up to $d_1/d_2 = 10^{-2}$, decreases slowly up to $d_1/d_2 \simeq 10^{-1}$, and then decreases more quickly up to $d_1/d_2 \simeq 1$.

So, in this model, which should only be considered for illustration purposes, one may tentatively suggest that a bigger grain is properly covered by smaller grains from $d_1/d_2 = 0$ up to $d_1/d_2 \simeq 2 \times 10^{-2}$, in such a case conventional kinetic models could be applied. In Fig. 8, $d_{ZnO}/d_{Al_2O_3}$ intervals, calculated from Fig. 1, have been drawn for various mixtures by taking $d_{ZnO} = 0.6$ μm. Results found in the literature are also reported in Fig. 8. Despite the fact that tabular alumina consists of tablet-like crystals and that reactive

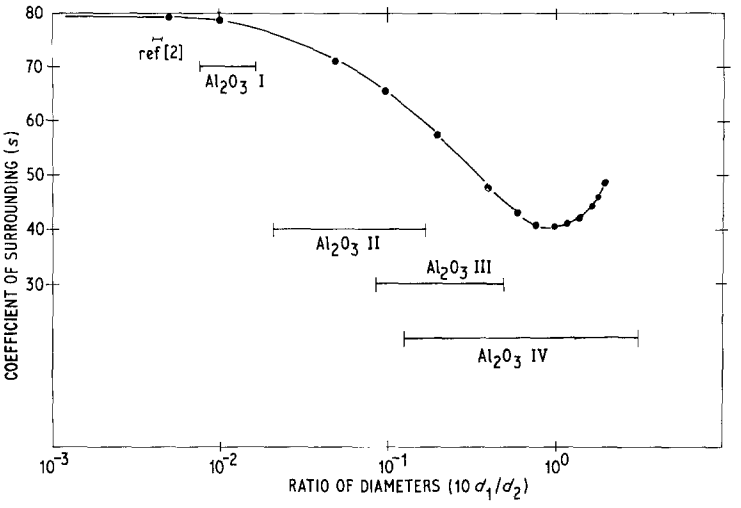

Figure 8 Evolution of the "coefficient of surrounding" against the ratio of sphere diameters.

alumina Al_2O_3 (IV) is in fact a mixture of non-reactive and reactive agglomerates, all shapes which are very different from spheres, the concept of the "coefficient of surrounding" enables us to separate the different kinetic behaviours. Above, the $d_1/d_2 \simeq 2 \times 10^{-2}$ geometrical factors appeared to be more and more important and models of kinetic powder reaction should take them into account. It is quoted in the introduction that in ceramics, as in other materials science fields, solid-state reactions are usually carried out by using fine powders in order to profit from their higher reactivity. Examination of the above results also shows that care must be taken in using fine powders of similar grain size in which reaction rapidly concentrates the product formed on portions of the host grain leading to difficulties in obtaining complete reaction.

References

1. W. D. KINGERY, H. K. BOWEN and D. R. UHLMANN, "Introduction to Ceramics" (John Wiley and Sons, New York, London, Sydney and Toronto, 1976) p. 42.
2. D. L. BRANSON, *J. Amer. Ceram. Soc.* **48** (1965) 591.
3. C. LEBLUD, M. R. ANSEAU, E. DI RUPO, F. CAMBIER and P. FIERENS, *J. Mater. Sci.* **16** (1981) 4716.
4. G. VALENSI, *Compt. Rend.* **202** (1936) 309.
5. L. MARGRAVE, "The Characterization of high temperature vapours" (John Wiley and Sons, New York, London, Sydney and Toronto, 1967) p. 497.
6. R. BEN AIM and LE GOFF, *Powder Technology* **2** (1968) 1.

Received 15 July
and accepted 1 August 1980

M. R. ANSEAU
F. CAMBIER
C. LEBLUD*
Centre de Recherches de
l'Industrie Belge de la Céramique
*and *Department of Materials Science,*
University of Mons,
15, Avenue Maistriau,
700 Mons, Belgium

A comparative study of the electrical resistivities of different finely divided carbon materials under compression

The influence of the nature of the filler and binder, the two main raw materials used in the manufacture of carbon products, on the characteristics of the latter is well established in the literature [1–4]. In particular, the filler is of paramount importance since it constitutes about 85% of the final carbon and graphite. For example, in a recent study [5] to determine the effect of the nature of the filler materials on the physical

0022–2461/81/041126–05$02.50/0 © *1981 Chapman and Hall Ltd.*